ULF WAVES OBSERVED WITH MAGNETIC AND ELECTRIC SENSORS ON GEOS-1

S. PERRAUT, R. GENDRIN, P. ROBERT, A. ROUX, and C. DE VILLEDARY

Département Etudes par Télédétection de l'Environnement, Centre National d'Etudes des

Télécommunications, 92131 Issy-les-Moulineaux, France

and

D. JONES

Space Science Department, European Space Agency Technology Center, Noordwijk, the Netherlands

Abstract. Preliminary results on ULF waves in the range 0.2–11 Hz detected on board GEOS-1 are described. In this frequency domain one must consider two different categories of emissions: waves with frequencies below the proton gyrofrequency f_{ci} and frequencies above. Belonging to the first category are the structured ULF events called 'pearls' which are very often observed on the ground, but which were observed only twice on board GEOS-1 in seven months of operation. Most of the monochromatic emissions with a frequency below f_{ci} were detected while the satellite was near its apogee $(L \approx 7)$. These waves are left hand polarized, perpendicular to the magnetic field. Other monochromatic events, whose frequency lies above the proton gyrofrequency are predominantly right hand polarized perpendicular to the magnetic field, whereas phenomena with complex, harmonically related structures, also detected above the proton gyrofrequency, are clearly polarized along the magnetic field. These waves can be probably interpreted in terms of Ion Bernstein modes.

We make here a morphological description of these different waves. We present preliminary results which relate their occurrence or characteristics to the parameters of the magnetospheric plasma. This study is mainly based upon data obtained via the magnetic detector although on some occasions, the electric component of the waves has been also identified and measured.

1. Introduction

GEOS is equipped with detection chains of magnetic and electric field fluctuations in the frequency range 0.05-11 Hz. This range covers three types of pulsations from low frequency to high frequency: Pc-3, Pc-1-Pi-1, and ELF waves. Taking into account the trajectory of the satellite (see in this issue the general introduction to GEOS where the orbital configuration is given), the proton gyrofrequency falls generally within the frequency domain detected by the sensors.

The study of Pc-3 is hampered by the fact that the spin rate of the satellite which is approximately equal to 0.18 Hz, has obliged us to introduce a filter at this frequency. The analysis of these waves is therefore more complicated than the analysis in the rest of the passband and we have not yet tried to study these waves, whose geophysical importance has however been stressed in a series of recent papers (see for instance Singer et al., 1977; Cummings et al., 1978; Hughes et al., 1978).

Since a long time intensive studies of Pc-1-Pi-1 have been carried out using ground data, and a classification of the different types of events which can be observed in this frequency range has been made based on their spectral shapes on

Space Science Reviews 22 (1978) 347-369. All Rights Reserved Copyright © 1978 by D. Reidel Publishing Company, Dordrecht, Holland

a three dimensional representation (Gendrin, 1970). Generally these pulsations observed on ground have frequencies below the minimum proton gyrofrequency along the field line and they are left hand polarized. One considers that these pulsations are ion cyclotron waves which can propagate along the field line at frequencies below the proton gyrofrequency.

Much was expected from direct in situ observations of these waves by means of satellites. The first measurements were carried out on board OGO-3 and -5. The trajectory of these satellites was such that they explored a large volume of the magnetosphere, leading Heppner et al. (1967, 1970) to find a Pc-1 distribution with a maximum near the magnetopause at the 6 hr local time meridian with high percentages extending tailwards near the magnetopause. Fredricks and Russell (1973) observed ion cyclotron waves in the polar cusp. Using data from Explorer 45, Taylor et al. (1975) found, on the contrary, about ten cases occurring near the plasmapause and in the proton ring current but they could not conclude that the waves were generated by the ion cyclotron instability or that the ion cyclotron waves played a dominant role in the loss of the ring current ions. A detailed comparison between the time of occurrence of these waves and the particle distribution functions led Taylor and Lyons (1976) to distinguish between two categories of waves: those which were associated with increasing fluxes of protons and those which were not. In fact the waves studied by these authors cover a wide frequency range (1–30 Hz) and no detailed spectral analysis of these waves was available. With a similar purpose in mind and with a similarly poor spectral information, Kintner and Gurnett (1977) have looked at records from Hawkeye 1. Only five events (over a period of 18 months) were detected and they were confined to the plasmasphere.

A statistical study of the occurrence of Pc-1 recorded on ATS-1 as a function of the local time and the magnetic activity was reported by Bossen *et al.* (1976a); these authors found a maximum in the afternoon sector at geostationary orbit. Comparison between ground measurements in the conjugate area and on board ATS-1 led the authors to conclude that most of the events detected in situ are IPDP's with a rather large amplitude (Bossen *et al.*, 1976b); this result is in agreement with the preferential occurrence of pulsations around 18:00 LT.

Waves with frequency above the proton gyrofrequency have been detected in the magnetosphere. These pulsations were considered to belong to the ELF range by Russell *et al.* (1970). The events observed on board OGO-3 occur only in the outer plasmasphere ($L \approx 4$ –5) and are confined near the magnetic equator (Russell *et al.*, 1970). These waves are propagating perpendicular to the magnetic field. Similar phenomena were detected at $L \approx 2$ –3, on board IMP-6 and Hawkeye-1 by Gurnett (1976) who shows clearly the harmonic structure of such emissions. Gurnett confirmed the strict localization of this noise near the magnetic equator.

Another type of electrostatic (or quasi electrostatic) noise attributed to plasmapause gradients has also been detected by Kintner and Gurnett (1978) in the frequency range above the proton gyrofrequency.

As appears from the above review of results obtained with the different satellites in the frequency domain covering 0.2–30 Hz, we can conclude:

- (1) Few emissions were observed due to the insufficient sensitivity of the on board sensors.
- (2) No precise information on the spectral characteristics of the phenomena (monochromaticity or wide spectrum for example \cdots) has been brought out due to the lack of systematic spectral analysis.
- (3) No unambiguous classification (based upon the morphological properties or on the mechanism of generation) has been defined so far.

As we will see in Section 2 where our magnetic experiment is briefly described, the sensitivity of our own equipment is much better than the ones used previously. In that section, the analysing method which leads to a systematic three dimensional representation (frequency, time, intensity) is also described.

In the following sections, we will give successive examples of magnetic phenomena with a frequency below the proton gyrofrequency (Section 3), then above the proton gyrofrequency, (Section 4). Some examples of the relationships which exist between the occurrence of the characteristics of the ULF emissions and the variations of the plasma parameters are given in Section 5. The last section is devoted to examples of electric signals some associated with magnetic fluctuations and some not.

on

A

he

en

of

ors

ese

or

om

ney

the

ese

bit.

ard

are

in

d in

nge

the

ssell

eld.

1 by

ons.

olas-

the

or.

2. Description of the Magnetic Experiment

For the detection of the magnetic fluctuations, in the ULF/ELF range, there are three orthogonal magnetic sensors whereas the electric signals are detected only on one component measured with the long radial boom E_y (see Figure 1 in S-300 experimenters, 1978). The magnetic component aligned along the spin axis is called B_z (in fact there is a small angle, $\approx 0.8^{\circ}$ between the z antenna and the spin axis so that this antenna is slightly affected by the rotation of the satellite, especially in the inner parts of the orbit where the DC magnetic field is strong). The two other components in the plane perpendicular to the spin axis are called B_x and B_y . The frequency sampling of these signals is ≈ 23 Hz, giving a Nyquist frequency ≈ 11.7 Hz.

Before going into the details of the treatment applied to these three signals, it is important to consider the sensitivity curves of the magnetic chain (see Figure 3b of Jones (1978)). A comparison with the sensitivity curves of ATS-6 and Explorer-45 shows that our ULF/ELF sensors operate with a better sensitivity ($\approx 2 \times 10^{-3} \, \gamma \, \text{rms Hz}^{-\frac{1}{2}}$ at 2 Hz) than the others (more than a factor 10). The notch which appears at the spin frequency (in the antenna reference system) is due to the special despin system which is incorporated within the S-300 magnetic ULF unit to attenuate the spin modulated component due to the DC field which would have otherwise saturated the telemetry dynamics range (70 dB). This despin system plays simply the role of a filter whose central frequency is synchronized to the

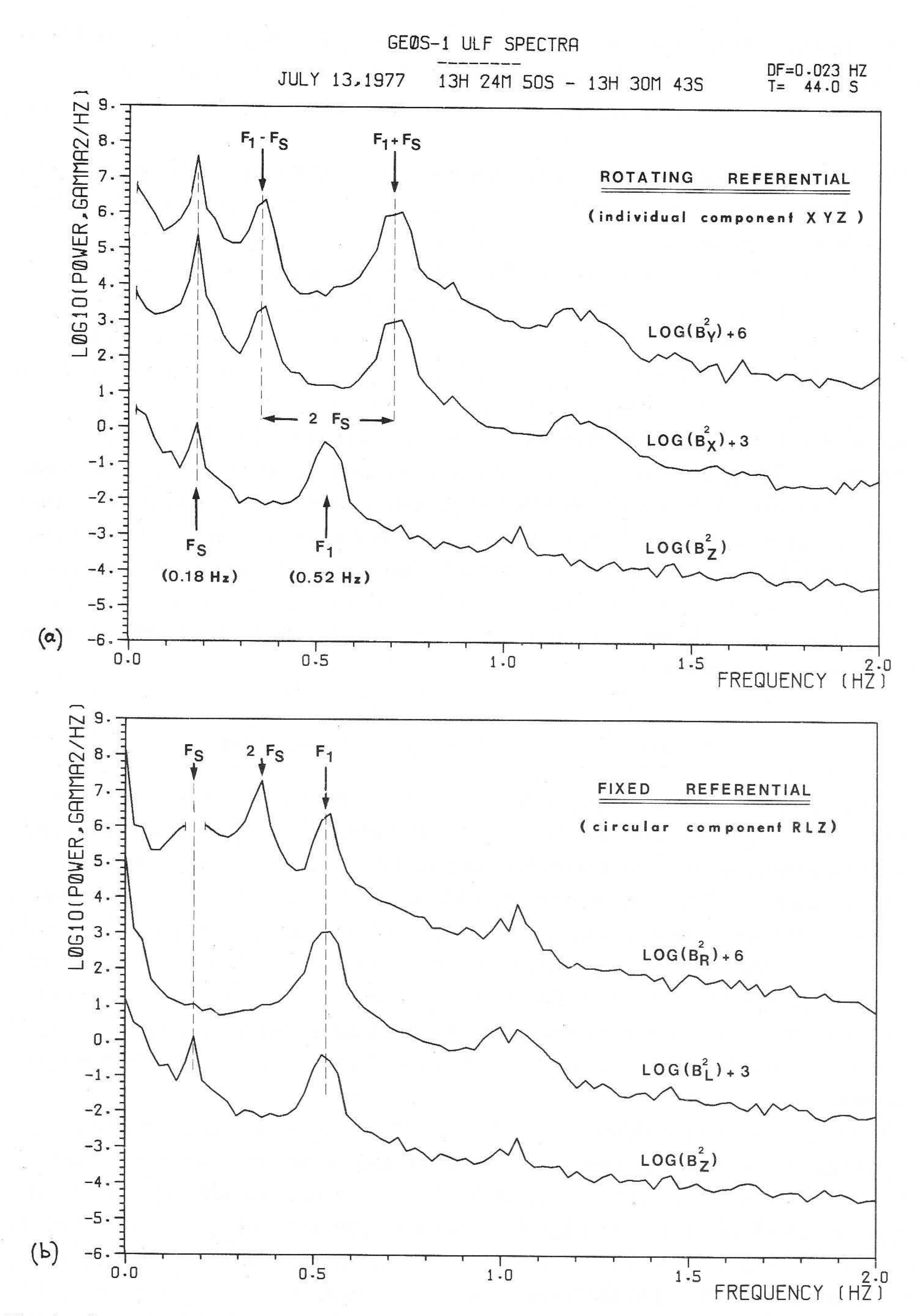


Fig. 1. Spectra of the three components of the ULF signal. (a) B_x , B_y , and B_z in the antenna reference system, B_z being aligned (to within 0.8°) along the spin axis. In spite of the despin system, the three components present a parasitic signal at the spin frequency F_s . An emission at F_1 appears on the B_z component, whereas the energy in splitted into two signals at $F_1 \pm F_s$, on B_x and B_y . (b) B_L , B_R , and B_z in a stationary frame of reference, B_L and B_R , being the circular components of opposite polarities. Now, the emission appears at the same frequency on the three components.

spacecraft spin. The attenuation is of the order of 26 dB, insufficient however to remove completely the strong influence of the DC magnetic field during the inner part of the GEOS-1 trajectory.

Signals are detected in the antenna reference system (upper part of Figure 1). Parasitic peaks at the spin frequency F_s appear on the three components in spite of the despin system. One must note on this figure that the emission during this period of time has a unique frequency F_1 on the B_z component which is almost unaffected by the satellite spin whereas the energy is split into two parts at the frequencies $F_1 \pm F_s$ on the orthogonal components B_x and B_y . It is more interesting to consider a stationary frame of reference and to distinguish between left hand (B_L) and right hand (B_R) components. This has been done applying Kodera et al. (1977) method with which complex modulation effects induced by the spin are easily removed by just a translation in frequency. The result obtained with such a method is represented in the lower part of Figure 1. The natural emission is seen now at the same frequency F_1 on the three components. The signal at the spin frequency has almost disappeared whereas a small component at $2F_s$ remains on B_R (which corresponds to the sense of rotation of the satellite at that time).

The advantages and difficulties of this analyzing method are explained elsewhere (Robert et al., 1979). It has been systematically applied to the ULF/ELF data on a routine basis. Spectra were computed over 512 points (i.e. 22 s). The transfer function of the chain and the gain factor of the step amplifiers (which can take the values 5, 25, and 125) were also taken into account. The results are plotted as a grey-scaled representation in the range 0–1.5 Hz as it can be seen on the next pictures. We must also mention that a complementary picture is also systematically generated. It consists of integrated powers of the signal in different frequency ranges up to 11 Hz plotted as a function of time. Evaluation of the amplitude is more precise on this second view.

It must be noted since now that the electric signal being detected only along one direction E_y , it is impossible to work with circular components to eliminate the rotation influence. Conversely, knowing the frequency of the signal by comparison with the magnetic emissions, it is possible to obtain an information on the polarization of the electric waves. If the magnetic pulsations are not observed simultaneously, it is not easy to exploit directly the electric data.

The two complementary pictures described above which are called 'experimenter summaries' were generated on a routine basis, in real time by the ESA Operation Centre in Darmstadt. The French Centre National d'Etudes Spatiales also performs off-line computation on these same data and provides us with two dimensional or three-dimensional pictures covering different frequency bands. All this set of analyzed data has been used for making the study which will be presented now.

3. Magnetic Emissions with $f < f_{ci}$

ntenna

system,

ears on

 $B_{\rm L}, B_{\rm R},$

pposite

Pulsations in the Pc-1 range commonly observed on the ground generally present

a typical structure called 'pearls'. On board GEOS-1 this characteristic spectral shape was observed clearly only two times over seven months of 'experimenter summaries' data. However this small number may be due to the limited time and frequency resolutions used in these summaries. A study, now in progress, made on more elaborate displays seems to indicate that the number of structured events may be slightly larger. One of these examples is shown on Figure 2 (upper panel). The repetition period of the order of 150 s is larger than expected at this distance $(R/R_e \approx 4.5)$ and for this frequency $(f \approx 1.2 \, \text{Hz})$, especially if one takes into account that a repetition period of 150 s at the level of the satellite corresponds to a repetitive period of $\approx 300 \, \text{s}$ on the ground.

In fact the spectral shape presented by most of the fluctuations observed on our records is given on the lower panels of the Figure 2. It consists of monochromatic emissions without clear repetitive structures. The duration of such events can be long (more than 3 hr on Aug 31, 1977). The wave frequency can be stable although the satellite is crossing various L shells. A study of the simultaneous appearance of these emissions at different ground stations is done elsewhere (Gendrin *et al.*, 1978).

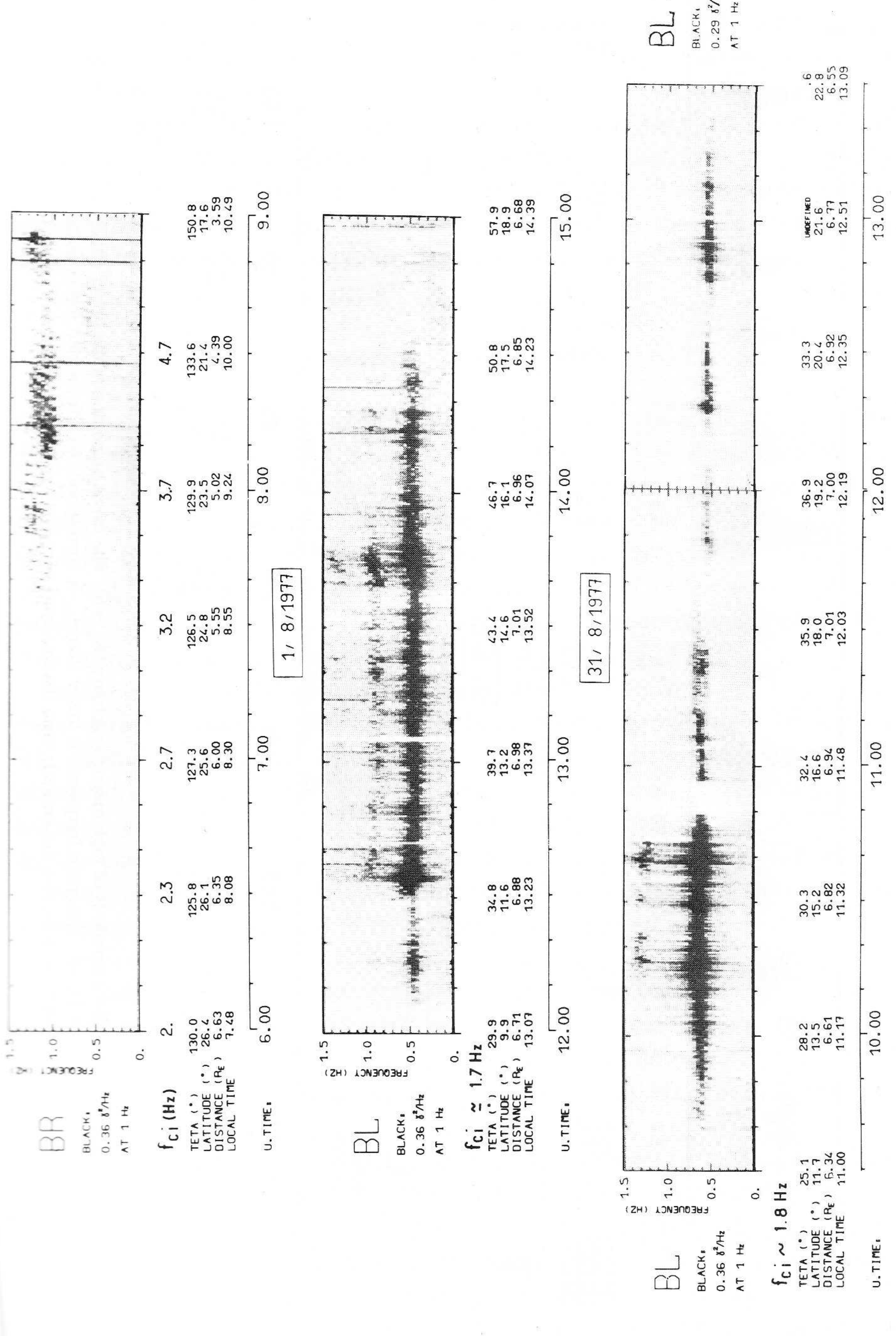
Sometimes a noise with more or less wide spectrum is superimposed as appears around 10:15 UT on the Aug 31, 1977 event. The origin of the harmonic structure seen on these spectra is not yet known, but we know that it is not due to a saturation of the detector because the amplifiers were in their lowest gain.

Events presented in Figure 2 are typical of quiet magnetic activity. During periods of high magnetic activity $(K_p \approx 6)$, bursts of noise are detected. They present a repetition period $\approx 10-20$ mm (see the upper event of Figure 3).

Oscillations similar to Irregular Pulsations of Diminishing Periods (IPDP), Auroral Agitation (AA) and Short Irregular Pulsations (SIP) observed on the ground are also observed on board GEOS. An example of SIP is given on the lower panel of Figure 3.

Up to now, no precise statistics on local time of occurrence, amplitude, polarization were developed for the different types of phenomena. But a first examination of the data leads us to the following conclusions:

- (1) Many ULF events have been detected in the magnetosphere (over a seven month period, we have observed ≈ 180 cases of Pc-1, ≈ 150 SIP's, ≈ 30 bursts events, characteristic of high magnetic activity and 4 IPDP's).
- (2) For monochromatic emissions, the average amplitude varies between 0.3 and 1γ at 0.5 Hz, explaining why similar events were scarcely observed on previous satellites.
- (3) Many events were observed around apogee, i.e. outside the plasmasphere. However we must note that the cold plasma density, as measured by the active wave experiments on board GEOS-1 (see for instance Etcheto and Bloch (1978) and Decreau *et al.* (1978a)) was very high (\approx 10–20 cm⁻³) at large radial distances, at least during the morning sector explored by GEOS-1 orbit during these seven months.



g

ι.,

to

ley

P),

the

the

ıde,

first

≈30

0.3

on

sma-

y the

3loch

adial

uring

7,12,1977

L

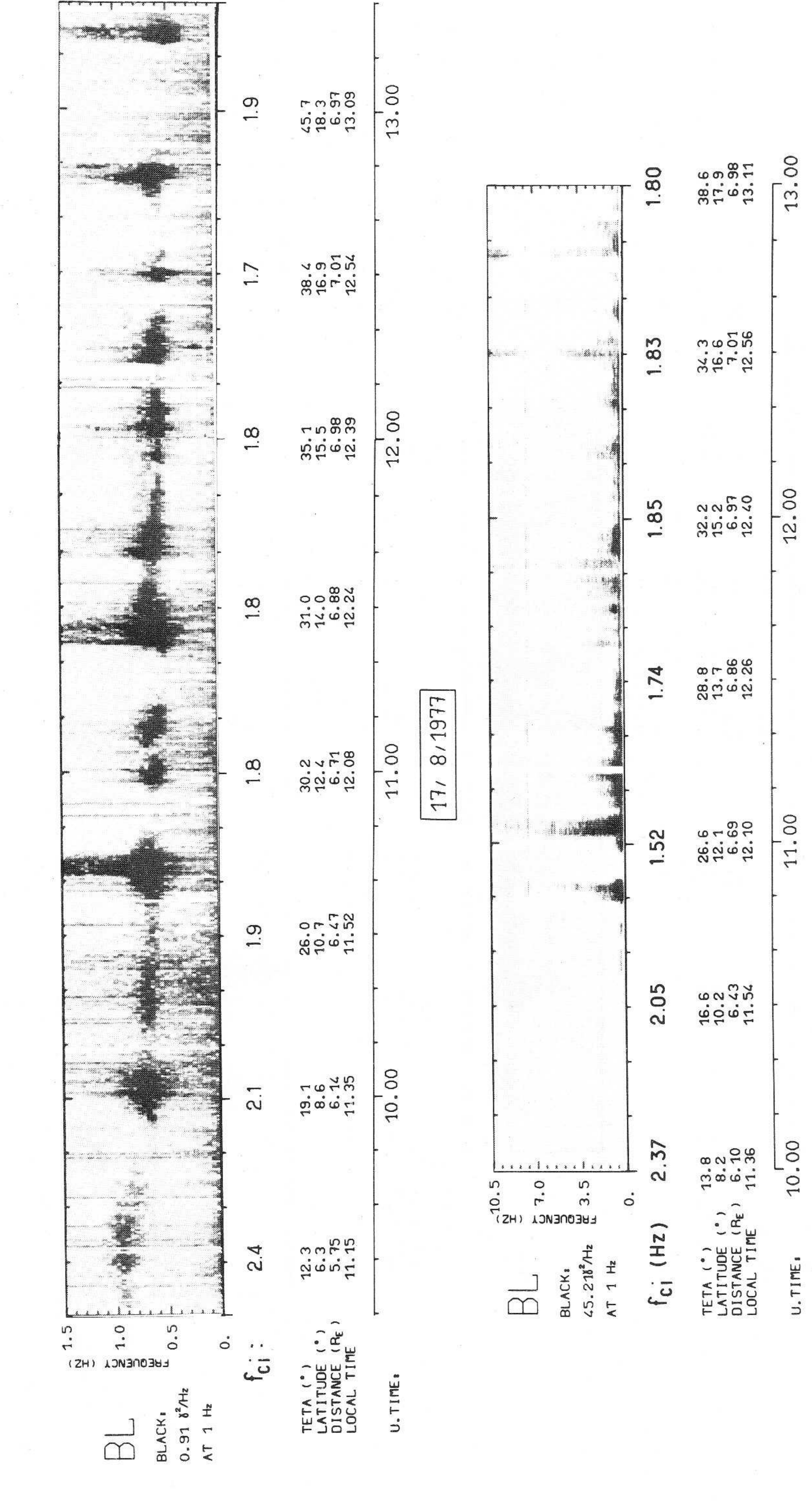
GEUS

emission long experimental of the tv The other two examples are presented to illustrate one represents (not due of faint harmonics upper panel The emissions. presence event). and the of quasi-monochromatic ULF Fig. 2. Typical spectra of quasi-monochromatic with a clear repetition structure (classical 'pearl' at a constant frequency

1977

18

S



event presented local wave cyclotron to left handed corresponds activity lower main frequency is of high occurring during periods 10 mn. looks like order the the lower panel a repetition period Fig. 3.

- (4) The mean ratio between the frequency of the monochromatic emission and the local proton gyrofrequency is of the order of 0.3.
- (5) Although it is difficult to characterize the wave polarization, because the angle θ between the spin axis and the magnetic field B_0 often is large, the B_L and B_R components of these $f < f_{ci}$ emissions have a larger amplitude than the B_z component.

In this section, we have considered SIP's because they are observed on the ground and that a fraction of their spectrum is less than f_{ci} . But in some circumstances, emissions with wide spectra clearly extending above the proton gyrofrequency are detected in space as we will see in the next section which is devoted to phenomena above the proton gyrofrequency.

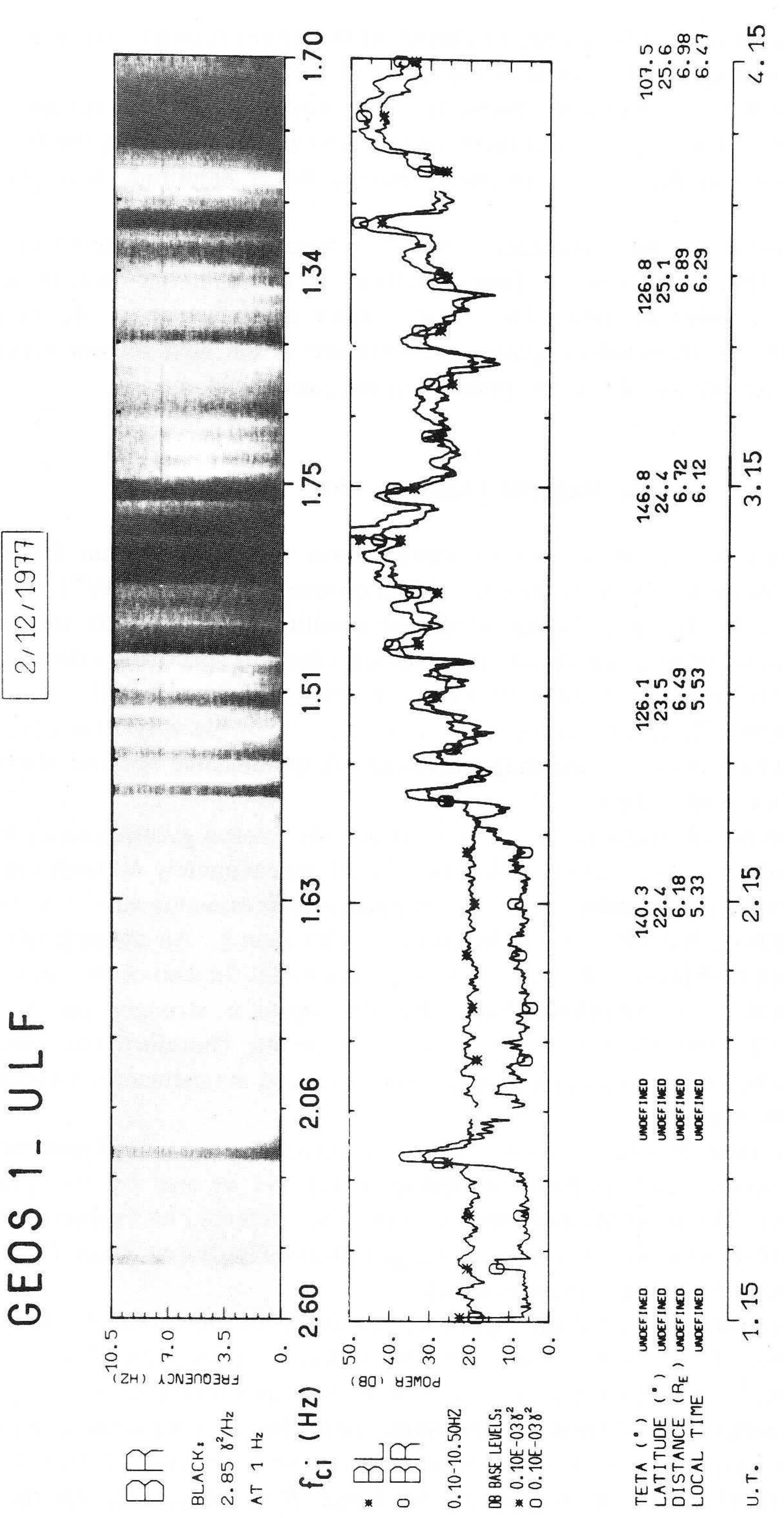
4. Magnetic Emissions with $f > f_{ci}$

On two occasions, the magnetopause compression was so large that GEOS-1 crossed the magnetospheric boundary. This happened on July 29, 1977 and on Dec 2, 1977. At the time during which the satellite was located in the magnetosheath, noise of large amplitude and with a continuous spectrum, extending at least up to 10.5 Hz (the Nyquist frequency of our equipment is \approx 11.7 Hz) was observed (Figure 4). These emissions are characteristic of the very strong plasma turbulence which occurs in the magnetosheath. A quantitative spectral study of this turbulence is in progress.

Different types of magnetic fluctuations above the proton gyrofrequency have been detected on board GEOS-1. We have listed approximately 40 such events. The most simple ones consist of a single monochromatic emission similar to those observed below f_{ci} but with a mean frequency higher than f_{ci} . An example of such events is given on Figure 5. It presents a fine structure (at the end of the emission) as do classical Pc-1 pulsations. Note that the signal is stronger on the B_R component (B_L and B_R having the same black level). Therefore this kind of emission can be considered to be a right hand polarized magnetosonic wave near ion gyroresonance.

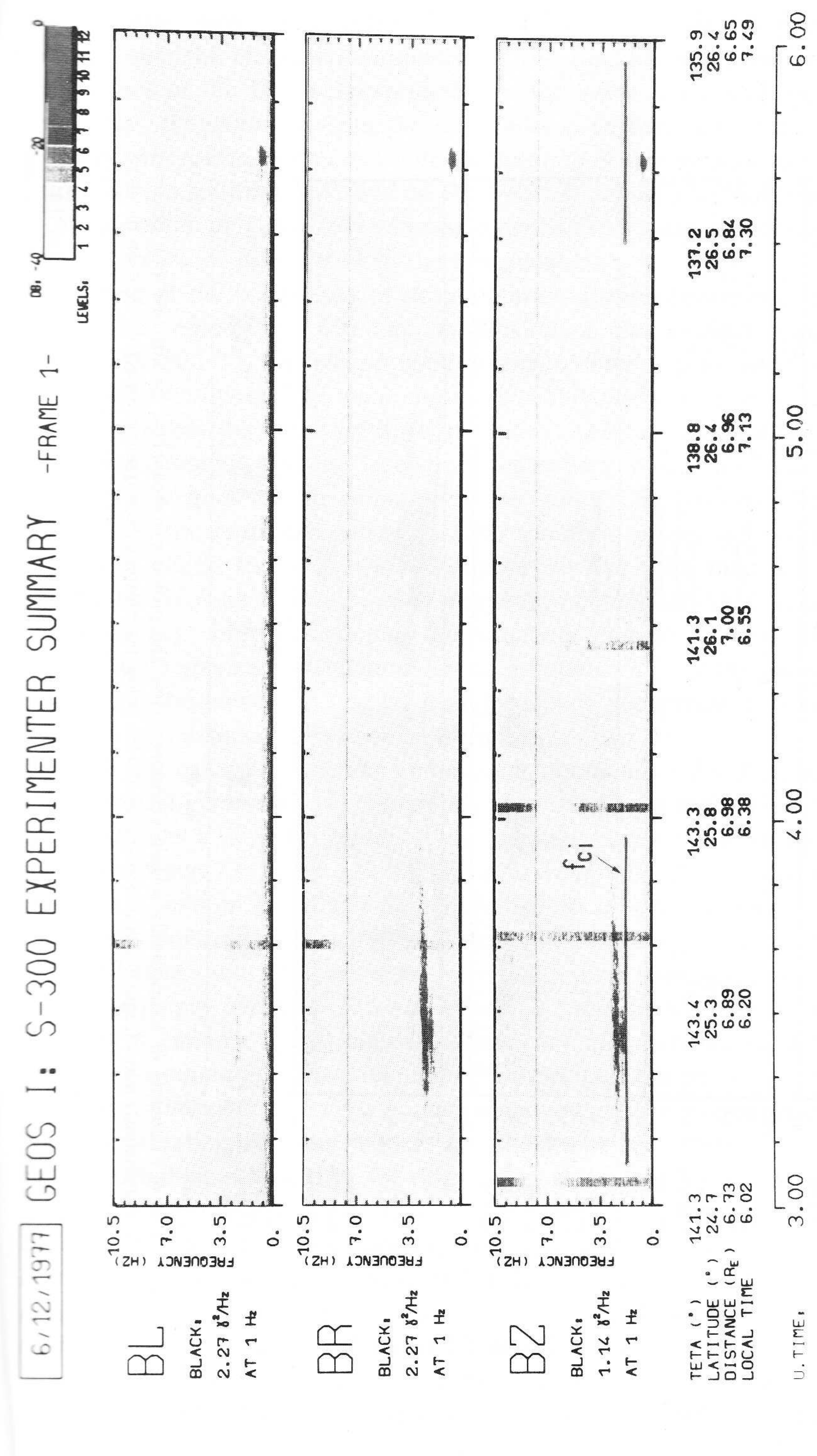
The other type of events presents a more complex structure. Generally it consists of several superimposed emissions separated or not by the proton gyrofrequency. These events look similar to the ones detected by Gurnett (1976) on board IMP-6, in a higher frequency range (30–100 Hz) but at lower L-values (2–3.5). Different cases are examined below.

In the examples presented on Figure 6, two different emissions are detected simultaneously. The emission around 0.4 Hz below f_{ci} (especially clear on the third panel from the top) is left handed polarized perpendicular to the magnetic field (B_L component) whereas, at the same time, higher frequency emissions composed of several harmonics (8 harmonics are visible around 14:50 UT) are clearly polarized along the magnetic field (large B_z). Occurrence on the B_L

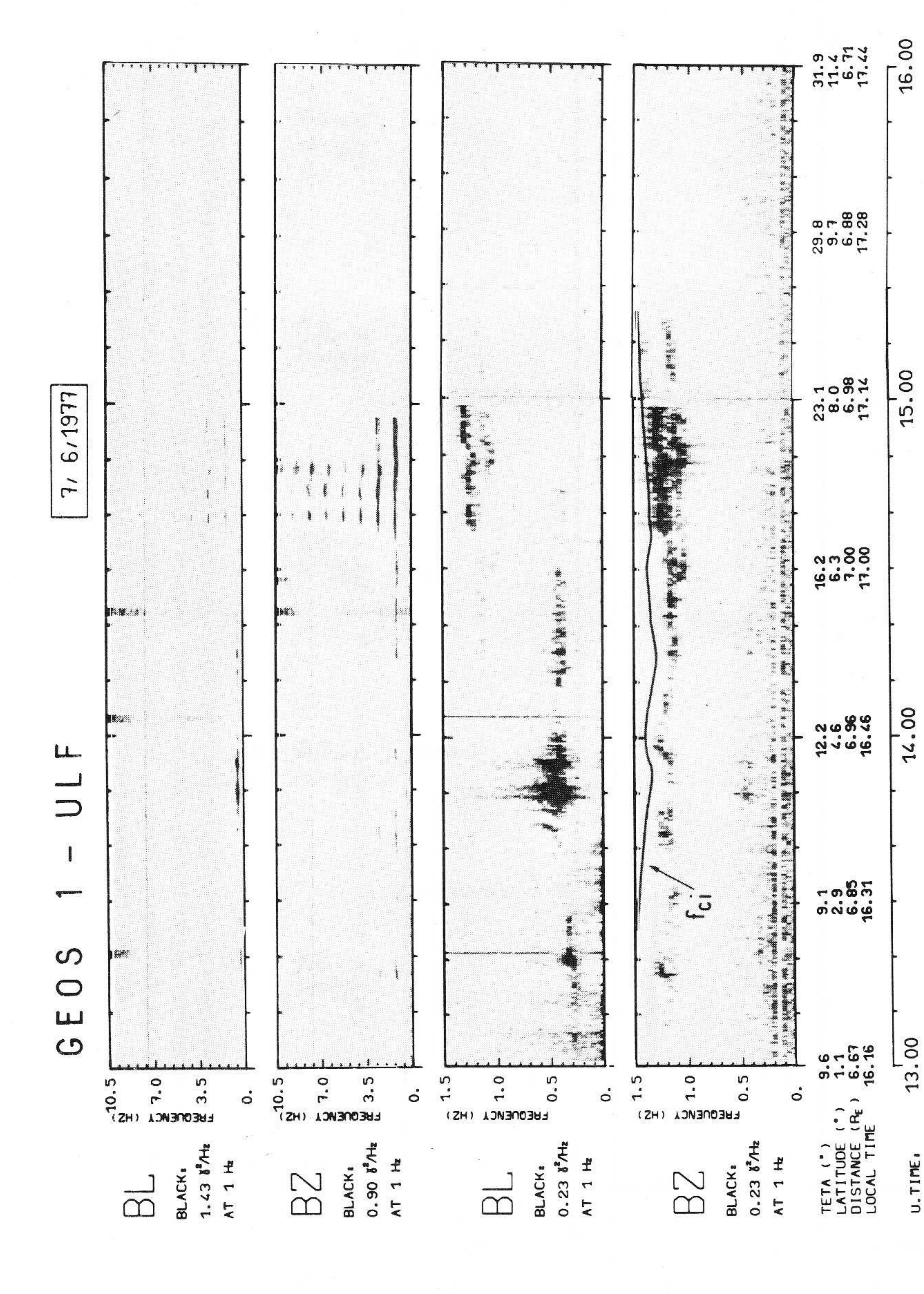


our transmitting equipment is typical of spectrum, which indicate a signal level the magnetosheath multiple crossings. Signals detected in this region have large amplitude (see the power curves below yquist frequency band. a continuous spectrum extending to the Ny (near 03:00), integrated in the whole f 10γ The December 2, 1977 event. This noise with as high as Fig. 4.

requency



almost magnetic than amplitude The two emissions between th compo emissions one sees that the emission below f_{ci} (around 05:40) presents a left mode of larger UT has a large right hand angle gyrofrequency. same distance. above the local proton The emission around 03:30 and below the proton gyrofrequency, approximately occur at the Example of a monochromatic wave observed equal for the two above



variations of the fundamental emission frequency seems to follow the proton gyrofrequency gyrofrequency left hand proton which different upper panel) the gyrofrequency. veral harmonically related emissions above frequency emission around 0.4 Hz below between the above emissions the separation related also harmonically simultaneously a low field field magnetic magnetic panel Fig.

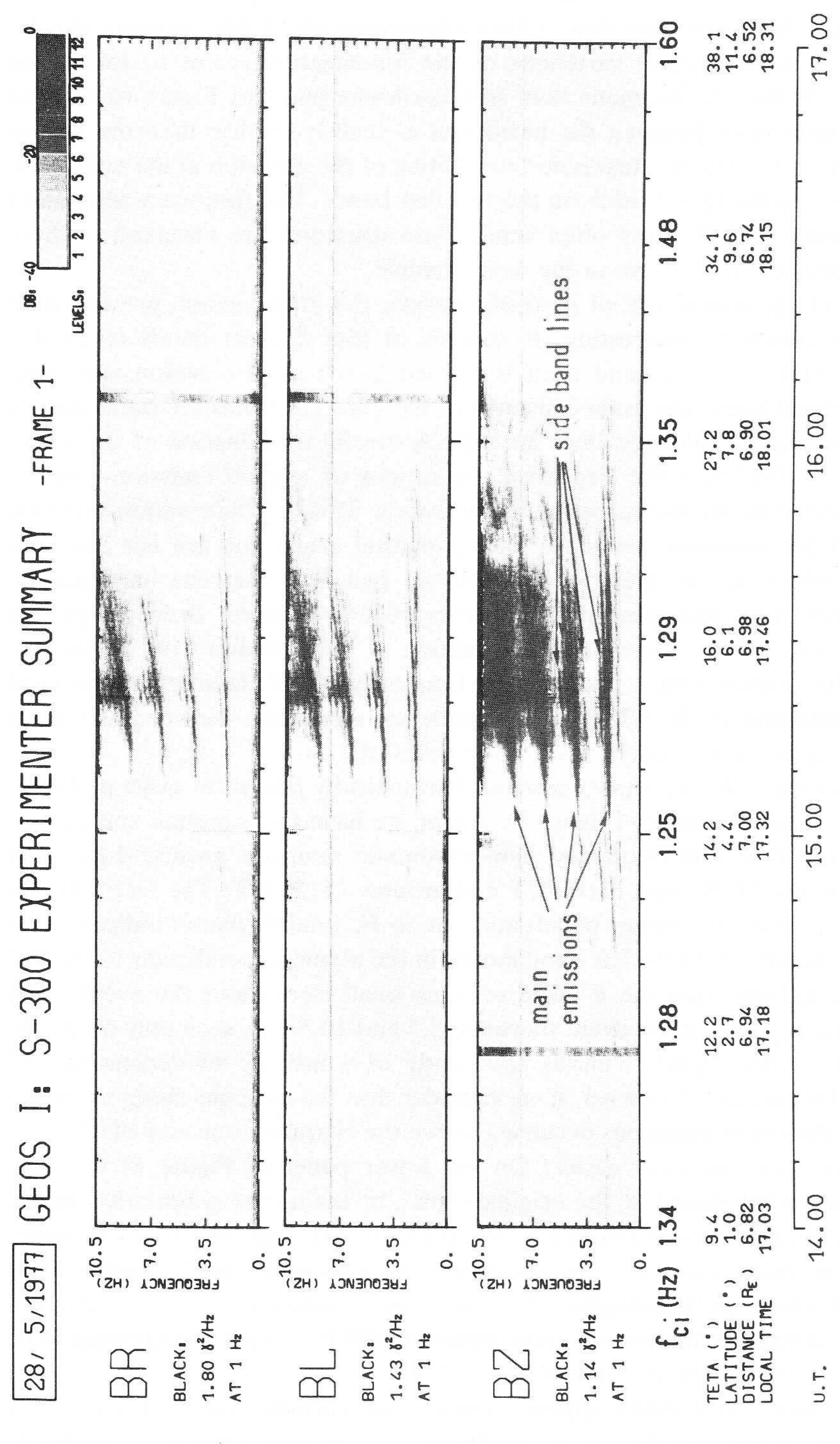
variations of the fundamental climssical variations of the differequency separation between the differequency The the

component after 14:30 UT is due to the fact that the θ angle (between B_z and the spin axis) increases with time. Other characteristics of this emission can be pointed out: the frequency variations of the fundamental seems to follow the fluctuations of the DC magnetic field (see the lower panel of Figure 6) and the frequency separation between the harmonics is slightly smaller than the proton gyrofrequency. Finally we must note the splitting of the emission at the end of the event. Such a splitting is visible on the two first bands. The frequency separation is of the order of $f_{ci}/8$. Very often similar fine structures are observed in these banded emissions as is shown in the next example.

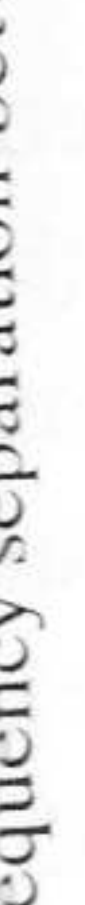
Because of the complexity of its configuration, the phenomenon presented on Figure 7 is especially interesting. It consists of four distinct bands (even five around 15:10 UT). Each band itself is divided into a main emission and some fainter sideband lines. The main emissions of the different bands are harmonically related whereas the sideband lines are not. A careful examination of the structures leads to find that the frequency separations of a main emissions and its adjacent sidebands are the same for all the bands. This last observation certainly proves that the harmonic emissions have a natural origin and are not due to a saturation effect. In the previous example we had seen that the harmonically related bands were multiples of a frequency slightly different from the proton gyrofrequency. In this example, the situation is even clearer: the bands are harmonically related with a fundamental frequency of ≈2 Hz whereas the local proton gyrofrequency is 1.3 Hz. The frequency separation between the main emission and associated sidebands are multiples of $f_{ci}/4$.

In the last example, we show emissions harmonically related at exact multiples of the proton gyrofrequency (Figure 8). Again, we have two simultaneous events. The first one is a low frequency monochromatic emission around 1 Hz seen mainly between 11:50 and 12:00 UT and around 12:25 UT. The fact that this emission is seen on B_L (upper panel) and not on B_z (middle panel) indicates that it is mainly polarized (in the left hand mode) in the plane perpendicular to the DC magnetic field (note that the θ angle remains small throughout the event). The higher frequency part of the event (between 3.5 and 10.5 Hz), seen only on the B_z component (middle panel) consists apparently of a mixture of decreasing and increasing frequencies. However, if we consider that the stronger rising tones are due to the aliasing of emissions occurring above the Nyquist frequency of 11.7 Hz, the interpretation becomes easier. On the lower panel of Figure 8, we have reconstructed what should be the original signal, by taking the symmetrical image with respect to the Nyquist frequency. We therefore see that the picture becomes coherent; the high frequency emission consists of a series of bands, harmonically related and which, in this example and within the accuracy of the measurements, are exact multiples of the proton gyrofrequency, which is slightly decreasing from 1.85 Hz at 12:00 UT to 1.55 Hz at 12:40 UT.

Although some differences appear between the various events with $f > f_{ci}$, it must be underlined that the emissions showing a harmonic structure are clearly



observation proves that lines are not sideband The main emissions are harmonically related, consists structure is composed of a main emission and of sideband lines. The main emissions are harmonically refrequency separation between sideband lines and the adjacent main emission is independent on the structuatequency separation between sideband lines and the adjacent main emissions which are not due to experimen This event emission. a harmonically related complex of a Example Fig.



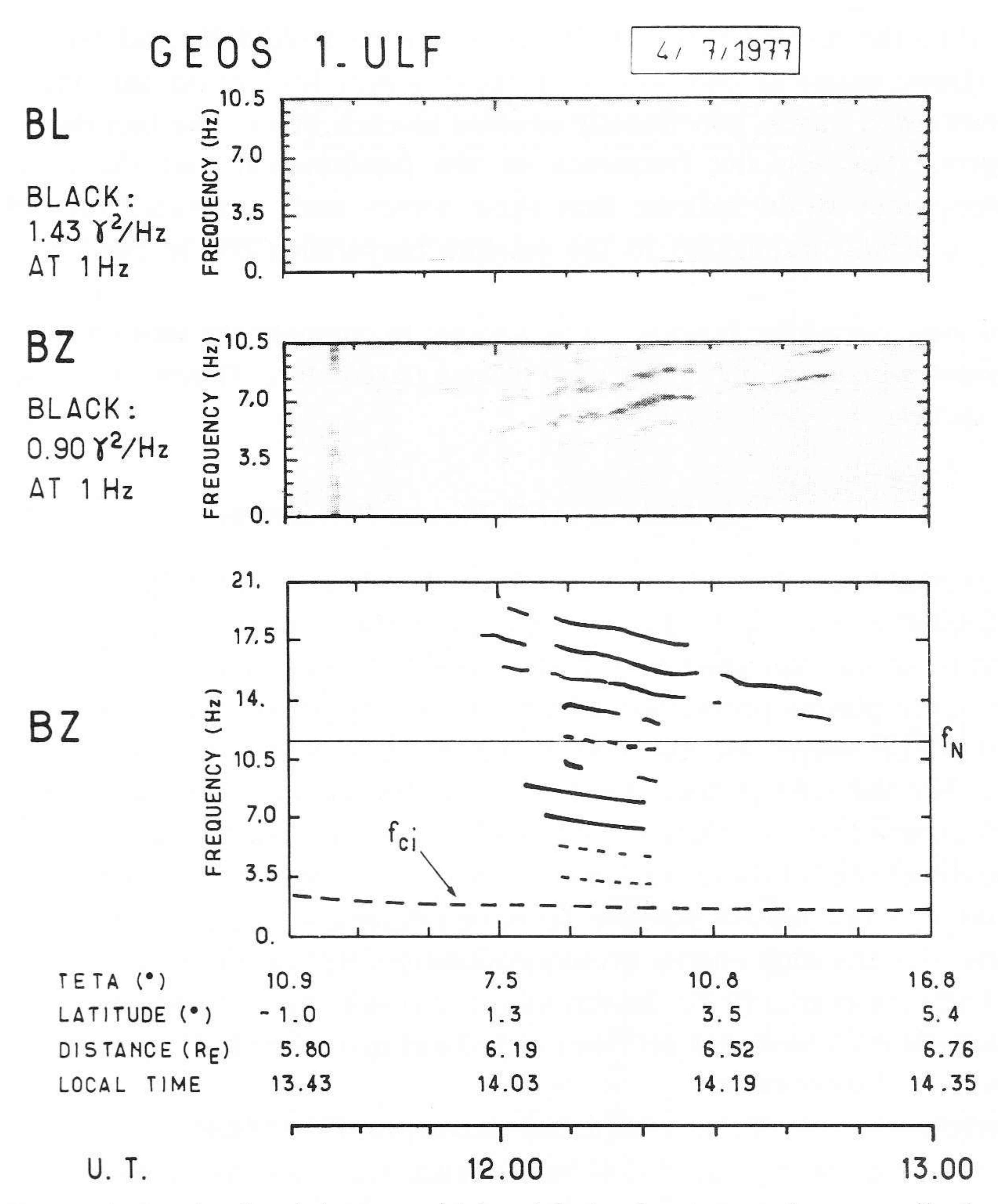


Fig. 8. Harmonically related emissions at multiples of the local proton gyrofrequency. On the upper panels are shown spectrograms of the phenomenon observed on B_L and B_z components. Again one observes simultaneously a low frequency emission below f_{ci} , which is left handed polarized perpendicular to the magnetic field (note that the θ angle is small) and higher frequency emissions polarized along the magnetic field. The experimental spectrum between 0 and 10.5 Hz is represented in the middle panel. After taking the image of the most prominent lines with respect to the Nyquist frequency, we obtain the schematic representations of the lower panel. Note that all the lines are harmonics of the fundamental frequency which follows the variation of the local proton gyrofrequency.

polarized along the magnetic field. Such waves cannot propagate along the field lines and this explains why they are so seldom recorded on the ground.

A first approach for the interpretation of these emissions is to identify them ion Bernstein waves (Kennel et al., 1970; Fredricks and Scarf, 1969; Cuperman and Gomberoff, 1977) but theoretical work has still to be done in understand better the different behaviour of these waves. If it were to understand, by further study, that the different bands are always at exact multiples of tendamental frequency, we should abandon the idea that these emissions are

related to the so-called $(n+\frac{1}{2})f_{ci}$ instability (Ashour-Abdalla and Thorne, 1977). The strong magnetic component of these waves lead us to interpret them as magnetosonic waves, non-linearly coupled to each other. The fact that there is a difference between the frequency of the fundamental and the local proton gyrofrequency could indicate that these waves were generated on different L shells and had propagated to the satellite perpendicularly to the DC magnetic field.

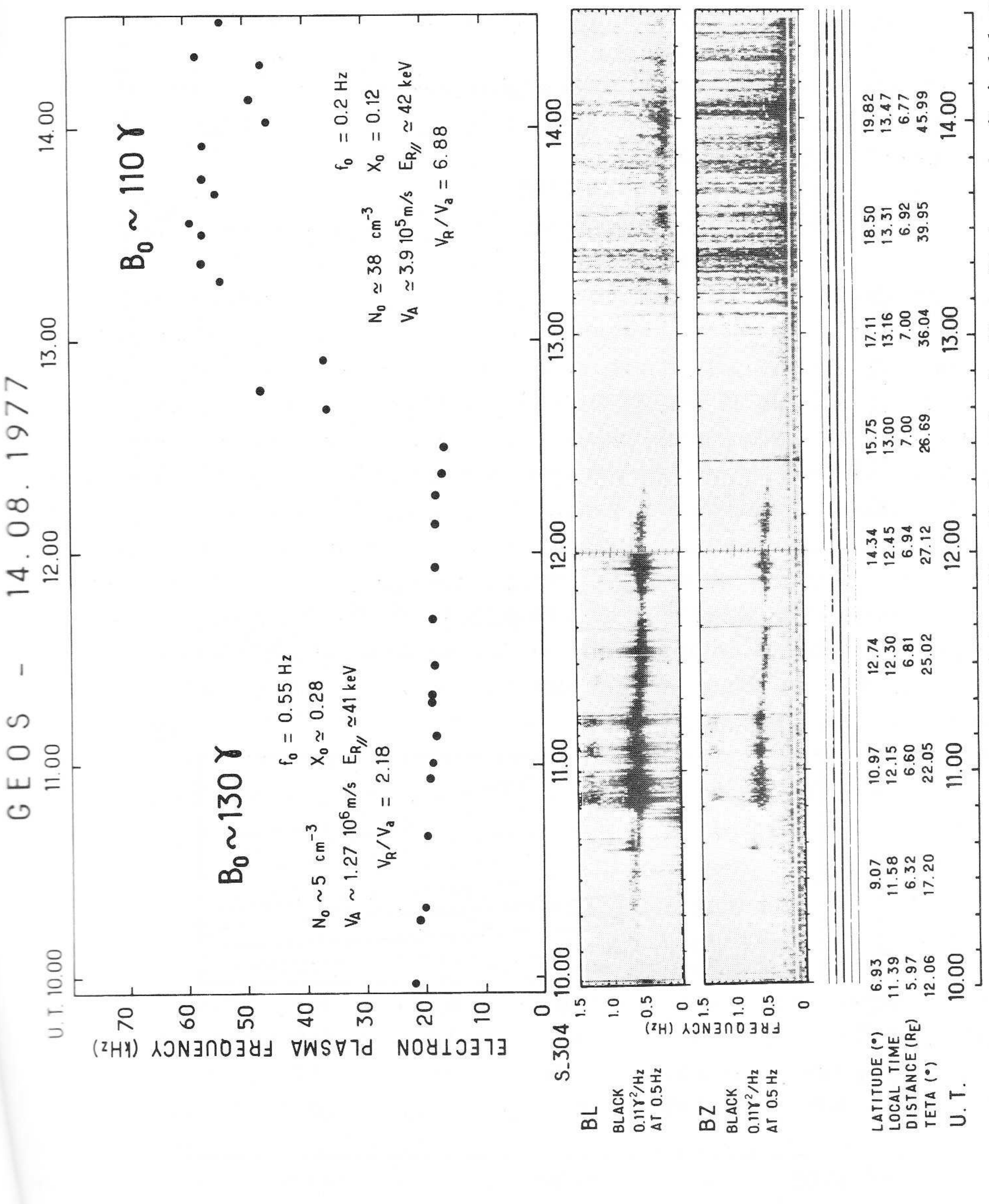
On some occasions, however, it is possible to compare the characteristics of the emissions with some important local plasma parameters. This is the subject of the next section.

5. Relation with Plasma Parameters

We present here some preliminary results obtained in trying to relate the characteristics of ULF emissions to the local plasma parameters as determined by other experiments on board GEOS. Besides the local proton gyrofrequency, the plasma parameters which play an important role in the amplification of ULF/ELF waves are the cold plasma density and the high energy particle fluxes. For the cold plasma density, we use the results of the active part of the S-300 experiment (see Etcheto and Bloch, 1978, and Decreau *et al.*, 1978a). One of the drawbacks of these experiments is that they are not continuously operating, so that it is not always possible to have detailed variation of the cold plasma density. For the high energy proton population, we use the result of experiment S-321 (Korth *et al.*, 1978). In this case the results are very preliminary because the particle data have not yet been sorted out according to their true energy and pitch angle distributions.

Studying the role of the cold plasma density on the appearance of ion cyclotron instability, Cornwall et al. (1970) have argued that such instability should preferentially take place within the plasmasphere. However a more refined study (Perraut et al., 1976) has shown that this should not always be the case if one takes into account the variation with L of the thermal energy and of the anisotropy of the hot particle population. The fact that the emissions below f_{ci} are mostly observed in the vicinity of GEOS-1 apogee is in agreement with this refined theory. Such an agreement is more easily understood if we note that the cold plasma density at these high L values ($L \approx 6$ -7) is indeed much higher ($n_c \approx 5$ -20 cm⁻³) than the values currently admitted ($n_c \approx 1$ cm⁻³) on the basis of measurements made with ion detectors whose results must in fact be considered cautiously (Decreau et al., 1978b).

The influence of the cold plasma density on the emitted frequency of the waves has also been considered. It is well known that the larger the cold plasma density, the lower the amplified frequency, assuming that the other parameters are constant. It has been possible to study such an effect on the August 14 event (Figure 9). Knowing the magnetic field B_0 obtained from the GEOS



e

e

nt

parallel colc 0 12:45 to be DC magnetic field intensity and the cold plasma The interacting electrons is found The density profile shows a noticeable increase around density. cold plasma with emission thermal energy of the cyclotron both the ion Variation of the central frequency of an The different central frequencies. Taking into accoun et al., 1978a). resonant energy ERII. impedance experiment (Decreau Fig. 9.

GEOS I - JULY 19, 1977

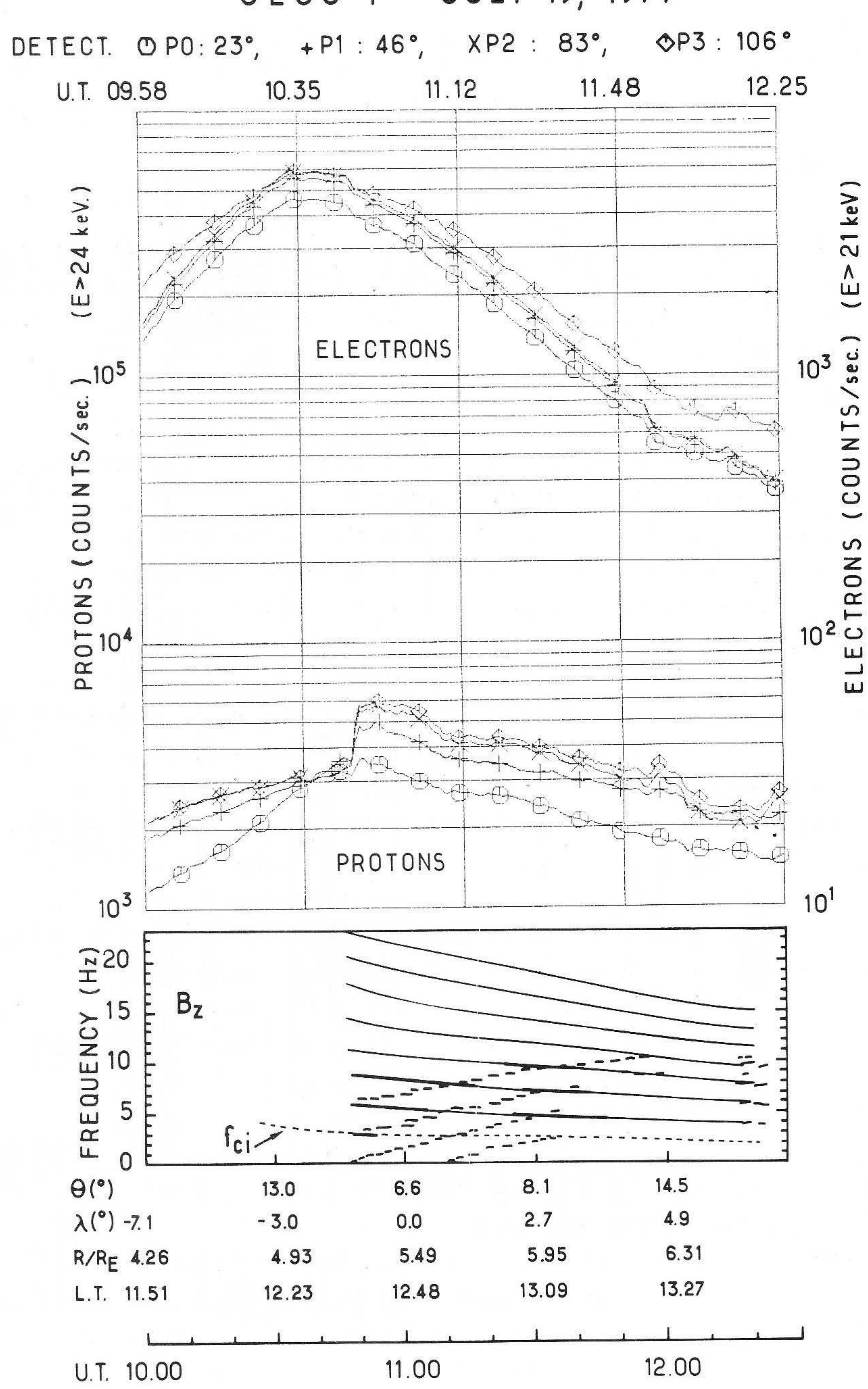


Fig. 10. Simultaneous increase of the proton flux and anisotropy and appearance of a harmonically related ULF emission. The angle θ between the spin axis and the magnetic field being small, the different angles quoted at the top of the figure for the different proton detectors correspond roughly to true pitch angles. The thick lines on the spectrogram correspond to the experimentally observed signal below the Nyquist frequency. The thin lines are obtained by a procedure similar to the one which was used in Figure 8. The emission is also polarized along the magnetic field.

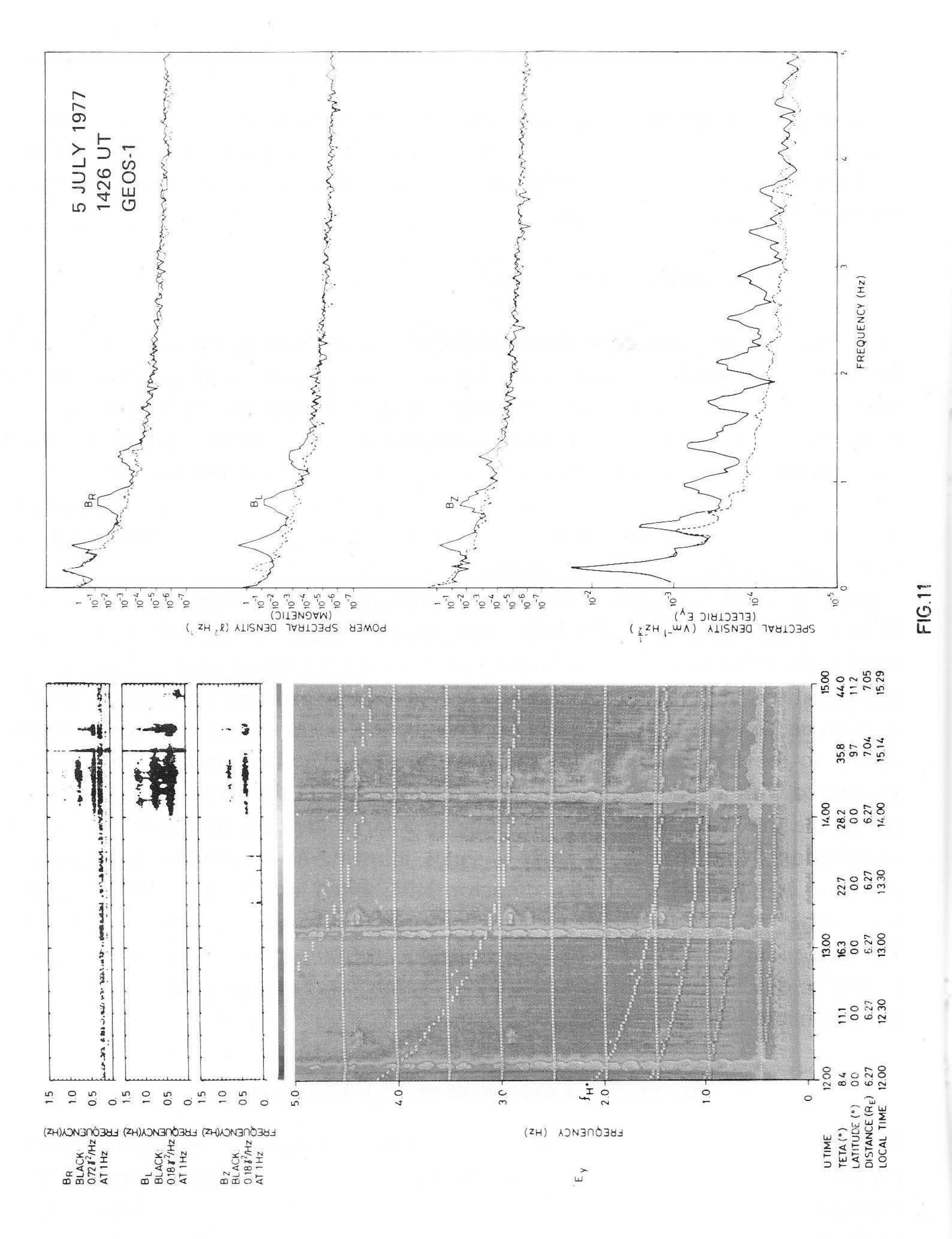


Fig. 11. ULF emissions seen in both magnetic (upper) and electric (lower) spectrograms between 14:00 and 15:00 UT, 5 July 1977. The harmonics in the magnetic channel are of natural origin, as is the harmonic structure in the electric channel. The intensity scale of the colour spectrogram is shown above, red being most intense. The dotted lines are the He⁺ and H⁺ gyrofrequency harmonics. The wide-band noise occurring every hour is of instrumental origin (bias sweep on spherical sensors).

Integrated spectra of B_R (right hand polarized), B_L (left hand polarized), B_Z (wave normal component) and E_y (electric signal) are shown on the right for the time indicated. The lower frequency components which appear in both magnetic and electric channels lie below the proton gyrofrequency. The higher harmonics seen only in the electric channel are probably ion-cyclotron harmonic waves.

The approximate threshold noise levels for the spectra are shown dashed.

fluxgate magnetometer and the cold plasma density n_e obtained from the mutual impedance experiment (Decreau *et al.*, 1978a), it is easy to deduce the Alfvén velocity V_A and the reduced frequency $x_0 = f/f_{ci}$. The parallel resonant energy is given by the following relation:

$$E_{R\parallel} = \frac{1}{2} m V_R^2 = \frac{1}{2} m V_A^2 \frac{(1 - x_0)^3}{x_0^2}.$$

With the data measured on board GEOS-1 for B_0 and n_e around 11:00 and 14:00 UT, one finds an equal value for the resonant energy ($E_{\rm R\parallel} \approx 40~{\rm keV}$). In both parts of the event $V_{\rm R}/V_{\rm A}$ is larger than 2. Therefore, provided that the anisotropy is larger than 1, the mean thermal velocity U_{\parallel} of the particle distribution function is almost equal to the resonant velocity (see for instance Figure 8 of Gendrin et al.'s (1971) paper). The change in the mean frequency of the emission can therefore be attributed solely to the change of the cold plasma density, the high energy proton thermal energy remaining constant.

From a rapid comparison with the proton data in the energy range above $20 \, \mathrm{keV}$ obtained from the S-321 experiments (Korth *et al.*, 1978), we have verified that there exist clear relationships between the occurrence of ULF waves and variations in the flux or anisotropy of high energy protons. A striking example is given on Figure 10. In this event high frequency, harmonically related emissions similar to those presented on Figure 8 are present. The beginning of the event is associated with a sudden increase of the integral flux in the direction perpendicular to the magnetic field, corresponding to a large increase in anisotropy of the distribution (Note that the θ angle is small, allowing us to consider the particles detected by the perpendicular detector have pitch angles near 90°). At the same time, no characteristic perturbation appears on the electron distribution. The same kind of particle fluctuations has not been observed in the other events. It may be due to the fact that we should look for lower energy protons ($<20 \, \mathrm{keV}$) for which the data are not yet available.

6. Electric Component of ULF Fluctuations

One electric component of ULF fluctuations is measured by the quasi-DC experiment employing the sensors at the ends of the long radial boom E_y . The experiment's sensitivity to ULF signals is shown inset in Figure 3a, 'Introduction to the S-300 Wave Experiment', this volume. The reduced sensitivity in the ULF range as compared to that at higher frequencies (>10 Hz) is a consequence of the requirement that the dynamic range be able to accommodate the relatively large induced at the spin frequency by the DC electric field. At the high the period of the ULF range, the sensitivity is further reduced by a low-pass which was included to avoid aliasing of signals above the Nyquist frequency relevant telemetry channel.

spectrograms are constructed by performing dynamic Fast Fourier Trans-FFT) on the signal. The example shown in Figure 11 illustrates an event

nically II, the ghly to signal ch was when both electric and magnetic ULF components are detected below the proton gyro-

frequency.

The frequency correspondence between the electric and magnetic components is somewhat obscured by the fact that with a single rotating electric antenna, signals are shifted in frequency by an amount equal to the spin frequency (0.17 Hz); the shift may be positive or negative depending on the sense of wave polarization. The red line at 0.17 Hz in Figure 11 represents the DC electric field which has been Doppler shifted from zero frequency.

It is seen in Figure 11 that the electric signal has a structure extending to higher frequencies, the waves being apparently located between harmonics of the helium

gyrofrequency.

These are probably ion cyclotron harmonic waves which have been reported to exist at low geocentric distances by Gurnett (1976) and Kintner *et al.* (1978); a theoretical approach to these phenomena has been recently made by Ashour-Abdalla and Thorne (1977).

On other occasions particularly during disturbed conditions signals detected on both electric and magnetic sensors extend up to high frequencies with no distinct harmonic structure. Both types of phenomena are the subject of further study.

Conclusion

We have presented here results which show that indeed the magnetosphere is very active in the ULF range. A large number of events have been recorded. The systematic spectral analysis of the events, associated with a polarization analysis, has allowed us to make a preliminary classification of these events. If we except the rare wide band events which are encountered when GEOS-1 was within the magnetosheath, all the events can be classified by their simultaneous frequency and polarization characteristics. Quasi-monochromatic emissions are mainly polarized perpendicular to the DC magnetic field. Often there is a mixture of left hand and right hand waves when $f < f_{ci}$, but when f is larger than f_{ci} the wave is generally polarized in the right hand mode. Emissions which present a harmonically related structure are mainly polarized along the DC magnetic field. The frequency of the fundamental emission may be above, below or at the proton gyrofrequency. Such emissions do often present sideband lines.

Preliminary results have been obtained on the relationships which exist between the ion cyclotron emissions $(f < f_{ci})$ and the cold plasma density. It has been shown that ion cyclotron waves generally occur near the GEOS-1 apogee, that is to say outside the dayside plasmasphere, in contradiction with previous theories. However the local cold plasma density is much higher than previously assumed for these large radial distances. On one example we were able to verify that the frequency of the emission was decreasing when the cold plasma density was increasing, and a quantitative estimation allowed us to check that the observed frequency was in agreement with the one we could deduce by assuming a constant distribution of high energy protons.

The conditions of generation of the harmonically related structures have not been studied in enough details. In particular, it would be interesting to have more measurements about the angular distribution of protons at energies below 20 keV. Similarly we should verify if these emissions are restricted to a well defined region around the geomagnetic equator as evidenced by Gurnett (1976) for low L-values.

Finally, a better understanding of the regions of the magnetosphere in which the low frequency emissions $(f < f_{ci})$ take place will be obtained by a comparison between ground and satellite measurements (Gendrin *et al.*, 1978).

Acknowledgements

We are grateful to Dr P. Decreau (Centre de Recherche en Physique de l'Environnement, Issy les Moulineaux, France), to Dr A. Korth (Max Planck Institute, Lindau, Germany) and to their colleagues for having provided us respectively with cold plasma density and high energy electron flux measurements.

We also acknowledge the work of Messrs M. Avignon and D. Forcioli (Centre d'Etudes Spatiales, Toulouse) who provided us with refined summaries of our ULF data.

References

Ashour-Abdalla, M. and Thorne, R. M.: 1977, Geophys. Res. Letters 4, 45.

Bossen, M., McPherron, R. L., and Russell, C. T.: 1976a, J. Geophys. Res. 81, 6083.

Bossen, M., McPherron, R. L., and Russell, C. T.: 1976b, J. Atmospheric Terrest. Phys. 38, 1157.

Cornwall, J. M., Coroniti, F. V., and Thorne, R. M: 1970, J. Geophys. Res. 75, 4699. Cummings, W. D., Deforest, S. E., and McPherron, R. L.: 1978, J. Geophys. Res. 83, 697.

Cuperman, S. and Gomberoff, L.: 1977, J. Plasma Phys. 18, 391.

Decreau, P., Beghin, C., and Parrot, M.: 1978a, Space Sci. Rev. 22, 581.

Decreau, P., Etcheto, J., Young, D. T., Wrenn, G. L., Pedersen, A., and Knott, K.: 1978b, Space Sci. Rev. 22, 633.

Etcheto, J. and Bloch, J. J.: 1978, Space Sci. Rev., 22, 597.

Fredricks, R. W. and Scarf, F. L.: 1969, in J. O. Thomas and B. J. Landmark (eds.), Plasma Waves in Space and Laboratory, University Press, Edinburgh. Vol. I, p. 97.

Fredricks, R. W. and Russell, C. T.: 1973, J. Geophys. Res. 78, 2917.

Gendrin, R.: 1970, Space Sci. Rev. 11, 54.

Gendrin, R., Lacourly, S., Roux, A., Solomon, S., Feigin, F. Z., Gokhberg, M. V., Troitskaya, V. A., and Yakimenko, V. L.: 1971, *Planetary Space Sci.* 19, 165.

Gendrin, R., Perraut, S., Glangeaud, F., Fargetton, H., and Lacoume, J. L.: 1978, Space Sci. Rev. 22, 433.

Gurnett, D. A.: 1976, J. Geophys. Res. 81, 2765.

Heppner, J. P., Sugiura, M., Skillman, T. L., Ledley, B. G., and Campbell, M.: 1967, J. Geophys. Res. 72, 5417.

Heppner, J. P., Ledley, B. G., Skillman, T. L., and Sugiura, M.: 1970, Ann. Geophys. 26, 709. Hughes, W. J., McPherron, R. L., and Barfield, J. N.: 1978, J. Geophys. Res. 83, 1109.

Jones, D.: 1978, Space Sci. Rev., 22, 327.

Kennel, C. F., Scarf, F. L., Fredricks, R. W., McGhee, J. H., and Coroniti, F. V.: 1970, J. Geophys. Res. 75, 6136.

Kintner, P. M. and Gurnett, D. A.: 1977, J. Geophys. Res. 82, 2314.

Kintner, P. M. and Gurnett, D. A.: 1978, J. Geophys. Res. 83, 39.

Kintner, P. M., Kelley, M. C., and Mozer, F. S.: 1978, Geophys. Res. Letters 5, 139.

Kodera, K., Gendrin, R., and de Villedary, C.: 1977, J. Geophys. Res. 82, 1245.

Korth, A., Kremser, G., Wilken, B., and Munch, J.: 1978, Space Sci. Rev., 22, 501.

Perraut, S., Gendrin, R., and Roux, A.: 1976, J. Atmospheric Terrest. Phys. 38, 1191.

Robert, P., Gendrin, R., Kodera, K., Perraut, S., and de Villedary, C.: 1979, Ann. Telecom., (to be published).

Russell, C. T., Holzer, R. E., and Smith, E. J.: 1970, J. Geophys. Res. 75, 755.

S-300 Experimenters: 1978, Planetary Space Sci., (to be published).

Singer, H. J., Russell, C. T., Kivelson, M. G., Greenstadt, E. W., and Olson, J. V.: 1977, Geophys. Res. Letters 4, 377.

Taylor, W. W. L. and Lyons, L. R.: 1976, J. Geophys. Res. 81, 6177.

Taylor, W. W. L., Parady, B. K., and Cahill, Jr., L. J.: 1975, J. Geophys. Res. 80, 1271.